# Polymer Chemistry

Accepted Manuscript


This is an *Accepted Manuscript*, which has been through the Royal Society of Chemistry peer review process and has been accepted for publication.

*Accepted Manuscripts* are published online shortly after acceptance, before technical editing, formatting and proof reading. Using this free service, authors can make their results available to the community, in citable form, before we publish the edited article. We will replace this *Accepted Manuscript* with the edited and formatted *Advance Article* as soon as it is available.

You can find more information about *Accepted Manuscripts* in the Information for Authors.

Please note that technical editing may introduce minor changes to the text and/or graphics, which may alter content. The journal's standard Terms & Conditions and the Ethical guidelines still apply. In no event shall the Royal Society of Chemistry be held responsible for any errors or omissions in this *Accepted Manuscript* or any consequences arising from the use of any information it contains.

ROYAL SOCIETY OF CHEMISTRY

www.rsc.org/polymers

# Construction of redox/pH dual stimuli-responsive PEGylated polymeric micelles for intracellular doxorubicin delivery in liver cancer

Hong Yu Yang [a,1], Moon-Sun Jang [b], Guang Hui Gao [c], Jung Hee Lee [b], and Doo Sung Lee [a,*]

[a] Theranostic Macromolecules Research Center, School of Chemical Engineering, Sungkyunkwan University, Suwon 440-746, Republic of Korea

[b] Department of Radiology, Samsung Medical Center, Sungkyunkwan University School of Medicine and Center for Molecular and Cellular Imaging, Samsung Biomedical Research Institute, Seoul 135-710, Republic of Korea

[c] Engineering Research Center of Synthetic Resin and Special Fiber, Ministry of Education, Changchun University of Technology, Changchun 130012, China

[*]Corresponding author :

Doo Sung Lee, Ph.D.

Theranostic Macromolecules Research Center, School of Chemical Engineering, Sungkyunkwan University, Suwon 440-746, Republic of Korea

Tel: 82-31-290-7297 / Fax: 82-31-292-8790； E-mail address: dslee@skku.edu

**Abstract**

A new type of redox and pH dual-responsive biodegradable polypeptide micelle was developed based on disulfide-linked methoxy poly(ethylene glycol)-b-poly[2-(dibutylamino)ethylamine-*L*-glutamate] (mPEG-SS-PNLG) copolymer and applied as an efficient and intelligent carrier to rapidly trigger intracellular release of doxorubicin (DOX). The mPEG-SS-PNLG was synthesized by a combination of ring-opening polymerization using mPEG-cystamine as a macroinitiator and a side-chain aminolysis reaction. The cumulative release profile of the DOX-loaded mPEG-SS-PNLG (DOX-mPEG-SS-PNLG) micelles indicated a low level of drug release (approximately 25 wt% within 24 h) at pH 7.4, which was significantly accelerated at a lower pH of 5.0 and a higher reducing environment (over 95 wt% in 24 h), demonstrating unambiguous redox/pH dual-responsive controlled drug release capability. In vitro cytotoxicity test indicated that empty mPEG-SS-PNLG micelles were nontoxic to HepG2 cells up to a tested concentration of 200 μg/mL. Confocal laser scanning microscopy observations revealed that DOX-loaded mPEG-SS-PNLG micelles efficiently released DOX into human hepatocellular carcinoma HepG2 cells following 24 h of incubation. Importantly, the DOX-loaded mPEG-SS-PNLG micelles significantly increased in vivo therapeutic efficacy toward HepG2 cells in comparison to the free-DOX and control groups. The successful demonstrations indicate that redox and pH dual-responsive mPEG-SS-PNLG micelles are a promising candidate for delivering anti-cancer drugs.

**Keywords:** drug delivery system, biodegradable, pH and redox dual-responsive, self-assembly, polypeptide

## Introduction

Over the last few decades, nano-sized micelles used in drug delivery systems have attracted widespread interest as one of the most promising platforms for cancer therapy.[1-5] In particular, particles with diameters smaller than 100 nm are effective in treating highly permeable tumors and enhanced accumulation at tumor sites as a result of their enhanced permeability and retention (EPR) effect.[6-8] In addition to the influence of small particle size, the long circulation time and stability of nanocarriers can also enhance retention efficiency.[9, 10] To achieve this goal, poly(ethylene glycol)ylated (PEGylated) micelles have been used to inhibit degradation in anticancer drugs, prolong drug circulation in blood and enhance drug accumulation in tumor tissue. Furthermore, PEGylated micelles have several additional advantages: they reduce drug side effects, improve drug tolerance, enhance micelle stability, and non-toxic and non-immunogenic.[11-13] In spite of these capabilities, nano-sized drug delivery systems still suffer from limitations. The main limiting factor is their uncontrolled drug release behavior after being injected into an animal or human body, which leads to insufficient drug accumulation at tumor sites.[14-16] To enhance the efficiency of drug delivery and achieve rapid release at tumor sites, many researchers have designed smart polymeric micelles whose drug release can be triggered in the tumor environment by internal or external stimuli-responsive conditions such as pH, redox chemistry, temperature, light, and magnetic fields, among others.[17-23] In particular, endosomal pH and cytoplasmic glutathione (GSH) have been designed and explored for enhanced cancer therapy.[24-27] It has been demonstrated that the pH can be as low as 6.0–7.4 in early endosome, then a later endosome (pH~5.5 to 6.0) and eventually 4.5–5.0 in lysosomes in cancer cells compared with approximately 7.4 in normal extracellular matrices and blood; additionally, the concentration of reducing glutathione (GSH) in the cytosol is 100-1000 times higher.[28-30] For

example, Chen et al. reported pH and reduction dual-sensitive polymers based on polyurethane materials and their derivatives. These polymers can self-assemble into stable micelles as carriers of imaging agents or drugs for detecting and/or treating tumors.[31, 32] Zhong et al. described novel redox- and pH- responsive micelles based on poly(ethyleneglycol)-SS-poly(2,4,6-trimethoxybenzylidene-pentaerythritolcarbonate) (PEG-SS-PTMBPEC) copolymers for DOX delivery.[33] Our group and Xing et al. reported a series of poly(β-amino ester) (PAE) copolymer, containing disulfide bonds in the backbone or side chain, which self-assembles into micelles in a physiological environment, and the micelles quickly release the loaded drugs in responding to tumor microenvironment.[34, 35] From the point of view of biomedical applications and facial polymer synthesis, controllable molecular weight, stability and biodegradability remain the essential requirements for drug delivery systems. It should be noted that side chain decoration is considered one of the most effective methods to embellish single polymers into multi-functional precursors. For instance, introduction of side chains with free reactive or functional ligands into polypeptides to enable more biomedical applications such as dopamine can be introduced act as anchor to stable iron oxide nanoparticles into biological systems.[36] Meanwhile, several groups have synthesized various series of functional polymer based on poly(benzyl-$_L$-glutamate) by a side chain aminolysis reaction, however, detailed information about the quantitative introduction of the functional groups by controlling reaction time or feed molar ratio were not report.[36-39]

Based on the reasons given above, we developed redox and pH dual-stimuli responsive biodegradable polymeric micelle based on methoxy poly(ethylene glycol)-cystamine-poly(2-(dibutylamino)ethylamine-$_L$-lutamate) (mPEG-SS-PNLG) diblock copolymers for efficient delivery of DOX into cancer cells. These novel dual-responsive polypeptide micelles were designed based on the following considerations: (i) polypeptides, which undergo reversible

secondary conformation transitions and/or hydrophilic–hydrophobic transitions in response to internal or external stimuli, are useful biocompatible and biodegradable polymers with structures that mimic natural proteins.[40-42] (ii) These polymers were synthesized via ring-opening polymerization (ROP) of α-amino acid N-carboxyanhydrides (NCAs) using initiators containing disulfide bonds of primary amines; the molecular weight can be controlled by changing the molar ratio of initiator to monomer.[43] Additionally, the pH sensitivity of the polymers was controlled based on the reaction time and/or feed molar ratio in a side-chain aminolysis reaction. (iii) As shown in Scheme 1, the antitumor drug DOX was loaded into the cores of nano-sized polymeric micelles for the purpose of accumulating at tumor sites by the EPR effect. After entering the tumor cells, nanocarriers would release the encapsulated drugs rapidly into the cytosol as a result of cleavage of the intervening disulfide bonds in the presence of a high GSH concentration and pH stimulus and resulting in the micelles rapidly dissolving, swelling or collapsing.

In this paper, the synthesis, in vitro drug release, cell uptake and antitumor activity of DOX-loaded mPEG-SS-PNLG micelles were investigated and the results indicate that these redox and pH dual-sensitive biodegradable micelles are highly promising tools for cancer therapy.

## Experimental materials and methods

### Materials

Doxorubicin hydrochloride (DOX), *L*-Glutamic acid γ-benzyl ester, 2-hydroxypyridine, anhydrous tetrahydrofuran (THF), anhydrous chloroform ($CH_3Cl_3$), anhydrous N,N-dimethylformamide (DMF), anhydrous dimethyl sulfoxide (DMSO), α-pinene, cystamine dihydrochloride, 4-nitrophenyl chloroformate (p-NPC), methoxy poly(ethylene glycol) (mPEG),

triethylamine (TEA), DL-dithiothreitol (DTT) and chloroform-d were obtained from Sigma-Aldrich (Germany) . Triphosgene and 2-(dibutylamino)ethylamine were purchased from Tokyo Chemical Hexane (Japan). Diethyl ether and ethanol were obtained from Samchun (Korea). All chemicals and solvents were used as received.

**Synthesis of macroinitiator methoxy-poly(ethylene glycol)-cystamine (mPEG-SS-$NH_2$)**

The macroinitiator mPEG-SS-$NH_2$ was synthesized as a reported in Zhong's work with slight modification (Scheme. 2a-b).[44] Briefly, (i) a round-bottom flask was filled with a solution of mPEG-OH (Mn=5000, 2 mmol, 10 g) and pyridine (10 mmol, 0.8 mL) in 60 mL of anhydrous DCM with vigorous stirring at 0 °C under a nitrogen ($N_2$) atmosphere. Then, 20 mL of DCM containing p-NPC (8 mmol, 1.61 g) was added dropwise to the reaction system. Finally, the reaction mixture was warmed to room temperature and allowed to react without interruption for 24 h. The activated mPEG was precipitated in cold diethyl ether after filtration and dried under vacuum for 72 h (Yield: 92 %). (ii) Under $N_2$ atmosphere, cystamine·2HCl (4 mmol, 0.81 g) and triethylamine (8 mmol, 0.81 g) were completely dissolved in 20 mL of anhydrous DMSO. Then, the solution was dropwise added to 10 mL of a DMSO solution of mPEG-NPC (0.4 mmol, 2 g) and stirred for 48 h at 30 °C. The macroinitiator mPEG-SS-$NH_2$ was obtained by extensive dialysis against a large amount of deionized water for 24 h to remove DMSO and unreacted small molecules, followed by lyophilization (Yield: 87 %).

**Synthesis of γ-Benzyl-$_L$-glutamate-N-carboxyanhydride (BLG-NCA)**

BLG-NCA was synthesized according to our previous work with slight modification[45] (Scheme. 2c). $_L$-glutamic acid γ-benzyl ester (10 g, 42.2 mmol) and α-pinene (11.47 g, 84.4

mmol) were suspended in 100 mL of anhydrous THF under a $N_2$ environment in a flame-dry three-neck flask. Then, triphosgene (6.255 g, 26.39 mmol) was dissolved in 10 mL THF and added slowly into the reaction mixture. The mixture was vigorously stirred at 55 °C until the milky solution turned clear within 0.5 h, and the reaction was allowed to continue for 2 hours. The product was precipitated by excess n-hexane and then purified by recrystallization in 3:1 hexane/ethyl acetate (v/v) twice (Yield: 96%).

**Synthesis of methoxy-Poly(ethyleneglycol)-cystamine-poly(benzyl-$_L$-glutamate) (mPEG-SS-PBLG)**

The mPEG-SS-PBLG was synthesized by ring-opening polymerization (NCA-ROP) of BLG-NCA with mPEG-SS-$NH_2$ as a macroinitiator (Scheme. 2d). Typically, mPEG-SS-$NH_2$ (1g, 0.19 mmol) and BLG-NCA (2.01g, 7.6 mmol) were dissolved in anhydrous chloroform using different molar ratios of initiator to monomer. Then, the reaction mixture was stirred under $N_2$ at 27 °C for 3 days. After the reaction was completed, the solution was precipitated into excessive cold diethyl ether. The collected white precipitate of the mPEG-SS-PBLG product was further washed twice with diethyl ether and dried in a vacuum oven for 72 h (Yield: 90%).

**Synthesis of methoxy-poly(ethyleneglycol)–cystamine–poly [2-(dibutylamino)ethylamine-$_L$-glutamate] (mPEG-SS-PNLG)**

mPEG-SS-PBLG was dissolved in anhydrous N,N-dimethylformamide (10 mL/1 g) under $N_2$ environment in a round-bottom flask and immersed in an oil bath at 55 °C. 2-(dibutylamino)ethylamine (10 × mol ratio to the benzyl groups of mPEG-SS-PBLG) and 2-hydroxypyridine (5 × mol ratio to the benzyl groups of mPEG-SS-PBLG) were subsequently

added. We obtained mPEG-SS-PNLG copolymers with different substitution ratios by varying the reaction time or changing the feed molar ratio of 2-(dibutylamino)ethylamine to benzyl groups. The resulting polymers were precipitated in cold diethyl ether. The final products were obtained after drying in a vacuum oven for 48 h (Yield: 82%).

The mPEG-SS-PNLG micelles were prepared by the pH-induced micellization method without the use of organic solvents. In detail, mPEG-SS-PNLG copolymers were added into phosphate-buffered saline (PBS) (pH 3.0) at the desired concentration. The solutions became clear by vigorous stirring. A 0.1 M NaOH aqueous solution was added to adjust the pH to 7.4, producing the mPEG-SS-PNLG micelles at a concentration of 1.0 mg/mL.

**Chemical structure**

The chemical structures of monomer and copolymers were characterized by $^{1}$H-NMR using a 500 MHz spectrometer (Varian Unity Inova 500NB) in deuterated chloroform ($CDCl_3$) containing 0.03 v/v of tetramethylsilane as a reference at room temperature. The different components of polymers were confirmed by checking the proton-peaks. The molecular weight (Mw) and polydispersity index (PDI) of the synthesized polymers were determined by GPC using 1 mg/mL of LiBr-containing DMF as eluent at 50 $^{\circ}$C and a flow rate of 1.0 mL/min. The molecular weights were calibrated using PEG standards.

.

**Acid-Base Titration**

The pH-buffering capacity of mPEG-SS-PNLG copolymer was measured by an acid–base titration method. Typically, 30 mg of mPEG-SS-PNLG copolymer was dissolved in 30 mL of deionized water and titrated to approximately pH 3.0. An acid–base titration curve was

constructed by adding 0.01 mL of 0.1 M NaOH dropwise to adjust the pH from 3.0 to 10.0 and recoding the pH. The pKa value of mPEG-SS-PNLG copolymer was estimated from the acid-base titration curve.

**Characterization of micelles**

The critical micelle concentration (CMC) of mPEG-SS-PNLG micelles were determined by fluorescence spectroscopy using pyrene as a polarity sensor. A pyrene buffer solution ($1\times10^{-6}$ M) was prepared by adding 1 mL of a solution of pyrene in THF (0.2 mg/mL) into 1 L of phosphate buffered saline (PBS) solution and evaporating the THF by heating at 60 °C for 6 h. The excitation spectrum of pyrene was fixed at an emission wavelength of 392 nm using a fluorescence spectrometer (AMINCO·Bowman, Series 2) at 25 °C. To obtain the CMC of mPEG-SS-PNLG copolymer, the concentration of mPEG-SS-PNLG copolymer (pH 7.4) in the pyrene-solubilized PBS was varied from 1 mg/mL to 0.002 mg/mL. The CMC was taken as the cross-point when extrapolating the intensity ratio $I_{337}/I_{334}$ at low- and high-concentration regions.

**Particle size and distribution of mPEG-SS-PNLG micelles**

The hydrodynamic radius and pH-responsive behavior of mPEG-SS-PNLG micelles at different pH values was measured by DLS (Malvern Instrument, Zetasizer Nano series, ZS90) with a helium laser at 633 nm and a digital correlator. The correlation function was accepted when the difference between the measured and the calculated baselines was <0.1%. The scattering angle was fixed at $90^{o}$ and before characterization, all mPEG-SS-PNLG micelle solutions were passed through membrane filters (pore size, 0.45 μm; Millipore). Transmission electron microscopy (TEM) was performed using a JEOL 1210 TEM operating at 100 kV;

images were recorded with a digital camera. The samples were prepared by dropping 10 μL of a 0.5 mg/mL suspension of the micelles on a copper grid without staining and blotting away the excess solution with a piece of filter paper.

**Redox sensitivity of mPEG-SS-PNLG micelles**

The redox sensitivity of mPEG-SS-PNLG micelles was measured by DLS at 37 °C. DTT medium (PBS, pH 7.4, 10 mM) was prepared with a polymer micelle concentration of 1 mg/mL. Micelle size changes were then monitored by DLS at different times (10 min, 30 min and 4 h) and the micelles in the absence of DTT were measured as a control.

**Drug Loading and Releasing**

DOX-loaded mPEG-SS-PNLG micelles were prepared as follows. Briefly, 5 mg DOX·HCl and twice the equivalent of TEA were mixed in 5 mL THF containing 50 mg mPEG-SS-PNLG. The mixture was allowed to stir at room temperature for 6 h in the dark. Then, 5 mL of deionized water was added dropwise to the solution under stirring. The mixture was stirred at room temperature for 2 h and the THF and free DOX were removed by dialysis against a larger amount of PBS solution (5 mM, pH 7.4) for 24 h to obtain DOX-loaded mPEG-SS-PNLG micelles. The solution was filtered through a syringe filter (0.45 μm, Millipore) and freeze-dried. The drug loading content (DLC) and the drug loading efficiency (DLE) of DOX-loaded mPEG-SS-PNLG were calculated based on the following equations:

DLE (wt%) = [weight of loaded drug/ weight of drug in feed]×100%

DLC (wt%) = [weight of loaded drug/ weight of drug-loaded micelle]×100%

In vitro release profiles of DOX from mPEG-SS-PNLG micelles were investigated using 50 mL centrifugal tubes containing 20 mL PBS at 37 °C under five different conditions, i.e.,: (i) PBS buffer solution (10 mM, pH 7.4), (ii) PBS buffer solution (10 mM, pH 5.0), (iii) PBS buffer solution (10 mM, pH 7.4, 10 mM GSH), (iv) PBS buffer solution (10 mM, pH 5.0, 10 mM GSH) and (v) PBS buffer solution (10 mM, pH 6.8, 10 μM GSH). A suspension of DOX-loaded mPEG-SS-PNLG micelles was added to cellulose ester membrane tubes (MWCO = 3500 Da). The cellulose ester membrane tubes were immersed into 20 mL of different PBS buffer solutions and shaken at 37 °C. At the desired time intervals, the cellulose ester membrane tubes were replenished with an equal volume of fresh medium. The concentration of DOX was determined by UV-visible spectroscopy (excitation at 479 nm).

**Cytotoxicity Evaluation**

Cell viability was examined using an MTT assay. Experiments were repeated at least four times at each concentration to obtain average values. Human hepatocellular carcinoma HepG2 cells were seeded onto a coated metal surface in each well (96-well plates) at 37 °C in MEM (Gibco, Grand Island, NY) containing 10% (v/v) of FBS (Gibco, Grand Island, NY) and 1% (w/v) of penicillin−streptomycin overnight (5% $CO_2$). Subsequently, empty mPEG-SS-PNLG micelles or DOX-loaded mPEG-SS-PNLG micelles were added into the wells to achieve different final concentrations. At 24 h post-treatment, the plate was shaken for a few minutes to thoroughly dissolve the dark blue crystals. The solution was then transferred to a 96-well plate and the absorbance was measured at 450 nm using Cell Counting Kit-8 (CCK-8, Dojindo, Kumamoto, Japan). The cell viability was calculated by comparing the MTT-treated cell solution with the control cell solution.

**Cellular uptake of DOX-loaded mPEG-SS-PNLG micelles**

In this investigation, the hydrophobic fluorescent agent DOX was selected to be encapsulated into the mPEG-SS-PNLG micelles for cellular uptake studies. Human hepatocellular carcinoma HepG2 cells were seeded on coverslips within 6-well plates ($1\times10^4$ cells/well) in MEM (Gibco, Grand Island, NY) containing 10% (v/v) of FBS (Gibco, Grand Island, NY) and 1% (w/v) of penicillin−streptomycin overnight (37 °C, 5% $CO_2$). Then, the cells were exposed to free DOX or DOX-loaded mPEG-SS-PNLG micelles (each with a DOX of concentration 10 μg $L^{-1}$) at 37 °C. After incubation for 1 and 24 h, the cells were fixed with 3.7% formaldehyde in PBS for 10 min, washed with PBS, soaked for 10 min in 3 mL of 4',6'-diamidino-2-phenylindole dihydrochloride (DAPI) and washed three times with PBS before being mounted on the slides. Cellular uptake was observed using a confocal laser scanning microscope (CLSM, LSM700 (CarlZeiss) X400) with a UV laser at wavelengths from 340 to 365 nm with excitation and emission wavelengths of 480 and 560 nm, respectively.

**In vivo antitumor activity**

The antitumor efficacy of DOX-loaded mPEG-SS-PNLG micelles was evaluated using subcutaneous tumor-bearing mice. BALB/c nude mice (21 ± 2 g; 6 weeks of age, Oriental Bio, Seoul, Republic of Korea) were managed according to the guidelines of the American Association for the Accreditation of Laboratory Animal Care and all animals also received care in compliance with the guidelines outlined in the Guide for the Care and Use of Laboratory Animals of the Korea, and all procedures were approved by the Animal Care and Use Committee of Samsung Biomedical Research Institute, Seoul, Republic of Korea. The animal model was

prepared by subcutaneous injection of hepatocellular carcinoma HepG2 cells ($1 \times 10^7$ cells per mouse). Drug treatment was initiated when tumor volumes reached ~100−200 $mm^3$, and the start day was designated as day 0. Three groups were formed with eight animals in each group: group I represented the control (normal saline-treated mice), group II consisted of free-DOX-treated mice, and group III consisted of DOX-loaded mPEG-SS-PNLG micelles-treated mice. The tumor-bearing mice were intravenously injected with 200 μL of treatment solution through the tail vein at a dose equivalent to a doxorubicin dose of 2 mg/kg body weight 7 times on day 0, day 3, day 6, day 9, day 12, day 15 and 18 day. A digital caliper was used for measuring tumor dimensions, and tumor volume was calculated using the following formula: $(width^2 \times length)/2$, where length represents the largest tumor diameter and width represents the perpendicular tumor diameter. On day 24 of the experiment, the mice were sacrificed, the tumor weights were measured and the tumor tissues were histologically evaluated via hematoxylin and eosin (H&E) and TUNEL staining (Promega Corp, WI).

### Statistical analysis

Data are expressed as the mean ± STD, statistical significance was determined using the Student's t-test. $P < 0.05$ was considered statistically significant, and $P < 0.01$ was considered highly significant.

## Results and discussion

### Synthesis and Characterization of mPEG-Cys, BLG-NCA, mPEG-SS-PBLG, and mPEG-SS-PNLG copolymers

A novel redox and pH dual-responsive mPEG-SS-PNLG block copolymer was synthesized through a four-step reaction (Scheme. 2). In the first step, the macroinitiator mPEG-SS-$NH_2$ was synthesized by activating the hydroxyl end group of mPEG (Mn=5.0 kg/mol) with p-NPC followed by treatment with an excess of cystamine in DMSO. The $^1$H NMR spectrum in $CDCl_3$ is shown in Figure S1. The results support a transformation of the hydroxyl end into cystamine as revealed by the existence of a peak at 2.91 ppm (corresponding to the methylene protons of a cystamine moiety lying adjacent to the disulfide bond) and 3.38 ppm (from the methoxy protons of mPEG). In the second step, BLG-NCA monomer was obtained at high purity after repeated recrystallization from an ethyl acetate/hexane mixture, and its structure was confirmed by $^1$H-NMR, as shown in Figure S2. In the third step, mPEG-SS-PBLG block copolymers were synthesized via typical ring-opening polymerization of BLG-NCA using mPEG-SS-$NH_2$ as a macroinitiator. $^1$H NMR exhibited characteristic signals corresponding to mPEG (δ 3.31 and 3.50 ppm) and PBLG (δ 5.1 and 7.3 ppm) (Figure S3), and the molecular weight and chain length of the block copolymer were found to be controllable by varying the molar ratio of monomer to initiator, with a higher ratio leading to a longer PBLG block (shown in Table 1). The degree of polymerization and molecular weight of mPEG-SS-PBLG were calculated by the integration ratio of peak f (the characteristic benzyl group peak) and peak b (the characteristic mPEG peak). And the weight average molecular weight (Mw) and PDI of the different chain length of the block copolymer were also determined by GPC (Table 1). In the final step, to obtain a pH-sensitive polymer, the benzyl groups of mPEG-SS-PBLG copolymer were substituted by grafting 2-(dibutylamino)ethylamine to the mPEG-SS-PBLG backbone (mPEG-SS-PBLG with a degree of polymerization of 40 [mPEG-SS-$PBLG_{41}$] was employed to maintain a hydrophobic/hydrophilic balance) with simultaneous debenzylation by an aminolysis reaction.

The 2-hydroxypyridine was added as a bifunctional catalyst into the reaction system during the aminolysis process to prevent chain scission of the polymer backbone (amide linkages of the polypeptide). The structure of mPEG-SS-PNLG was confirmed by $^{1}$H-NMR. As shown in Figure 1, we observed the near disappearance of peaks at 5.1 and 7.3 ppm (which were attributed to the benzyl groups of mPEG-SS-PBLG) and the appearance of peaks at 0.78, 1.3, 1.4 and 2.4 ppm (which were attributed to the butyl groups in the newly formed mPEG-SS-PNLG copolymer).

The conversion of benzyl groups can be controlled by varying the reaction time or the feed molar ratio of 2-(dibutylamino)ethylamine to benzyl groups. The corresponding structures of mPEG-SS-PNLG with different conversion were monitored using $^{1}$H-NMR (Figure S4a-b). The conversion of benzyl groups and molecular weight in mPEG-SS-PBLG$_{41}$ as a function of reaction time and as a function of feed molar ratio are shown in Table 2a and 2b, respectively. And the weight average molecular weight (Mw) and PDI of the different conversion copolymer also were analyzed by GPC (Table 2a and 2b). The relationship between the conversion and the reaction time is shown in Figure 2a, we found that the reaction rate was initially fast, with 39% of benzyl groups being replaced by 2-(dibutylamino)ethylamine. The reaction rate subsequently increased slowly because of the decreasing concentration of unreacted benzyl groups until 72 h, and almost all of the benzyl groups (96%) had been replaced. Interestingly, the conversion of benzyl groups can also be controlled by changing the feed molar ratio of 2-(dibutylamino)ethylamine to benzyl groups. As shown in Figure 2b, the conversion increased with increasing feed molar ratio and 96% of benzyl groups were replaced by 2-(dibutylamino)ethylamine when the feed molar ratio had been increased to 20:1. This is due to the increased reaction probability of 2-(dibutylamino)ethylamine to benzyl groups in a short

reaction time (24 h). These results indicated that we can obtain the desired conversion by controlling the reaction time or changing the feed molar ratio.

The solubility of mPEG-SS-PNLG copolymers was correlated with the percentage of benzyl groups converted. At conversion percentages lower than 70%, mPEG-SS-PNLG copolymers were not fully soluble in water even at low pH of 3.0. However, at conversion percentages higher than 75%, the polymers showed pH dependent solubility and could be dissolved in water at low pH (3.0). Especially, the mPEG-SS-PNLG(90%) copolymer showed suitable pH sensitivity and good stability at pH 7.4, comparing with the other mPEG-SS-PNLG copolymers with different conversion percentages. Thus, only mPEG-SS-PNLG(90%) copolymer was used to further study of drug delivery in this work.

**pH buffering capacity of mPEG-SS-PNLG**

The pH-buffering property of mPEG-SS-PNLG(90%) copolymer was determined using an acid-base titration method. As shown in Figure S5, the pH-buffering region of mPEG-SS-PNLG (90%) copolymer is broad with high conversion of benzyl groups because the higher content of tertiary amine groups leads to the consumption of more $OH^-$ groups, and increases the pH-buffering capacity. On the basis of the inflection points of the buffering curves, we have calculated the pKa value of mPEG-SS-PNLG(90%) copolymer and list it in Table 2a. The titration curve indicated that the pKa values of mPEG-SS-PNLG copolymers (Table 2a) also increased with increasing conversion of benzyl groups due to benzyl groups are more hydrophobic than 2-(dibutylamino)ethyl groups, mPEG-SS-PNLG copolymers with a higher percentage of benzyl group conversion exhibited higher pKa values.

**Characterization of mPEG-SS-PNLG(90%) micelles**

Polymeric micelles based on pH-responsive behavior could be prepared simply by changing the solution pH from 3.0 to 7.4 in the absence of organic solvents. The critical micelle concentration (CMC) is an important parameter to assess the stability of self-assembling polymeric micelles. The CMC value is defined as the intersection of the tangent point to the curve at the inflection with the horizontal tangent through the points at low polymer concentrations. As shown in Figure S6, we found that the CMC value was approximately 0.023 mg/mL for mPEG-SS-PNLG(90%) copolymer which is similar to the others mPEG-SS-PNLG copolymers of the CMC values (Table 2a) by fluorescence measurements using pyrene as a fluorescence probe in pH 7.4 PBS. The fluorescence intensities of pyrene in mPEG-SS-PNLG(90%) solutions of different polymer concentrations are shown in Figure S7.

**pH-responsive behavior of mPEG-SS-PNLG(90%) micelles**

The hydrodynamic sizes of these micelles were summarized in Table 2a at pH 7.4, which were all small, ranging from 58.0 to 66.0 nm. The pH-responsive behavior of mPEG-SS PNLG(90%) in aqueous media was investigated by DLS. As shown in Figure S8(A), we found that the hydrodynamic sizes of increased from about 62.0 nm to 150.0 nm with decreasing solution pH from 7.4 to 6.0. This result demonstrated that the micelles swelled because of the protonation of tertiary amine groups within the polypeptide segments, which made the micelle core less hydrophobic and the hydrophilicity of polypeptide segments was enhanced markedly, rendering the swelling of the aggregates. With the decrease of pH to 5.0, the micelles almost were damaged when the size of micelles down to about 10 nm. The pH-responsive behavior of mPEG-SS-PNLG(90%) micelles was further confirmed by using the zeta potential. It can be seen

from Figure S8(B) that the positive zeta potential increased with decreasing pH from 7.4 to 5.0, indicating that more tertiary amine groups are protonated with the decrease of the pH, leading to core of the micelles produce positive charged. It is noted that the positive charged core of the micelles and its capacity of disrupting endosomes, due to the proton sponge effects, may further promote the application of the micelles for cytoplasmic drug delivery.[46,47] Additionally, TEM micrographs indicated that these micelles exhibited a spherical morphology with particle sizes in accordance with those determined by DLS (Figure 3).

**Redox-responsive behavior of mPEG-SS-PNLG(90%) micelles**

The disulfide bond linkage between the hydrophobic and hydrophilic blocks is expected to exhibit redox-sensitive properties. The reduction-responsive behavior of mPEG-SS-PNLG(90%) micelles was investigated using DLS. The disulfide bonds in mPEG-SS-PNLG(90%) micelles were rapidly destroyed in a reducing environment containing 10 mM DTT at pH 7.4. The results showed that mPEG-SS-PNLG(90%) micelles quickly swelled from 62 nm to approximately 200 nm in 10 min after adding DTT to the solution, and micelle size further increased from 200 nm to 300 nm in 0.5 h and to over 1,000 nm in 4 h (Figure 4). This size increase is likely caused by the splitting off of the intervening disulfide bonds, which rapidly results in shedding of the hydrophilic part and aggregation of the hydrophobic part of the micelles[48]. Therefore, the reduction-sensitive property of mPEG-SS-PNLG(90%) micelles was confirmed when the micelles were rapidly dissociated in the presence of a high concentration of DTT.

**Drug loading and triggered release**

DOX, an anthracycline anticancer drug with red fluorescence, is widely used as the hydrophobic model drug for the treatment of multiple types of solid malignant tumors in the clinic.[49] DOX was loaded into the pH and redox dual-responsive mPEG-SS-PNLG(90%) micelles through the dialysis method. The DLC and DLE of DOX in the mPEG-SS-PNLG(90%) micelles were determined to be 7.2% and 58.6%, respectively. The size of DOX-loaded mPEG-SS-PNLG(90%) micelles was approximately 93 ± 6 nm, which is larger than that of empty micelles (Figure S9). The controlled drug-releasing behavior of the DOX-loaded mPEG-SS-PNLG(90%) micelles was investigated under different conditions, including (i) pH 7.4, (ii) pH 5.0, (iii) pH 7.4 and 10 mM GSH, (iv) pH 5.0 and 10 mM GSH and (v) pH 6.8 and 10 μM GSH . The cumulative release percentages of DOX loaded in mPEG-SS-PNLG(90%) micelles versus time are plotted in Figure 5. The results show that without the existence of GSH, the accumulative release of DOX in physiological (pH 7.4) buffer reached approximately 25% within 4 h, with no further release observed to 24 h time point. At a pH 6.8 and 10 μM GSH concentration condition (imitating the extracellular fluids environment where GSH concentration is approximately 2-20 μM and pH value is around 6.5-7.0)[50,51], a higher DOX was released by comparing with pH 7.4, the release amounts reached to about 45% after 24 h. this result suggests that redox and pH dual-responsive mPEG-SS-PNLG(90%) micelles increased drug release rate under extracellular fluids environment due to the partial ionization of tertiary amine groups, leading to the micelles swelled and released a partial of DOX. However, the DOX release rates were accelerated at acidic pH (pH 5.0) and over 80% of the loaded DOX was released in 24 h from the destabilization of micelles. In the presence of 10 mM GSH, the DOX release was accelerated and reached over 50% within 4 h and almost 85% after 24 h. The fastest and most complete drug release was observed at pH 5.0 in the presence of 10 mM GSH (imitating the

intracellular compartments, such as cytosol)[52] wherein approximately 95% of DOX was released within 24 h. The fast DOX release behavior from mPEG-SS-PNLG(90%) micelles under reducing conditions was most likely due to reduction-triggered cleavage of the disulfide bonds in the block junction of the hydrophilic and hydrophobic segments, leading to rapid and nearly complete DOX release, as the micelles destabilized.

These results clearly indicate not only that pH and redox dual-responsive mPEG-SS-PNLG (90%) micelles enable synergistic effects in drug release, but also that they can be selectively accumulated in tumor tissue by the enhanced permeability and retention (EPR) effect, which may enhance the overall therapeutic efficacy in vivo.

**In vitro cytotoxicity studies**

The in vitro cytotoxicity of blank mPEG-SS-PNLG(90%) micelles and DOX-loaded mPEG-SS-PNLG(90%) micelles was assessed using the MTT assay. The HepG2 (human hepatocellular carcinoma) cell line was used. Notably, the mPEG-SS-PNLG(90%) micelles showed no cytotoxicity against the HepG2 cells even at a concentration of 200 μg/mL **(**Figure 6**)**. It should be noted that the DOX-loaded mPEG-SS-PNLG(90%) micelles had highly toxic to HepG2 cells (cell viabilities < 40%) up to a tested concentration of 30 μg/mL. The results indicated that blank polymeric micelles are safe and biocompatible. Meanwhile, the DOX-loaded mPEG-SS-PNLG(90%) micelles were easily and efficiently taken up by the HepG2 cells and released DOX in an acidic and reduced intracellular microenvironments, which agreed well with the in vitro drug release behavior of DOX-loaded mPEG-SS-PNLG(90%) micelles.

**Cellular internalization**

To further demonstrate that the redox or/and pH responsive behavior of DOX-loaded mPEG-SS-PNLG(90%) micelles results in beneficial internalization by cells in the tumor environment, the cellular uptake behavior of DOX-loaded mPEG-SS-PNLG(90%) micelles was investigated in HepG2 cells by CLSM. As shown in Figure 7, after 1 h of incubation, the red fluorescence intensity of free DOX increased compared to DOX-loaded mPEG-SS-PNLG(90%) micelles because of its redox and pH dual-sensitivity, DOX-loaded mPEG-SS-PNLG(90%) micelles systematically entered to the cytosol followed by nucleus for effective cancer therapy. It is known that DOX exhibit anticancer property by inhibiting the growth macromolecular biosynthesis via intercalation with intracellular DNA.[53] With increasing incubation time (from 1 h to 24 h), fast internalization of DOX-loaded mPEG-SS-PNLG(90%) micelles and rapid release of DOX inside cells was found in comparison to the rate of free DOX, highlighting the efficient release of DOX promoted by the increased acidity and concentration of GSH in the tumor intracellular environment.

**Tumor suppression study of DOX-loaded mPEG-SS-PNLG(90%) micelles in vivo.**

Tumor growth inhibition with the DOX-loaded mPEG-SS-PNLG(90%) (DOX-loaded PMs) micelles formulation was evaluated in vivo in HepG2 liver tumor-bearing mice using tail vein injection. Mice were treated with free DOX and DOX-loaded mPEG-SS-PNLG(90%) micelles at a DOX dose of 2 mg per kg of body weight; normal saline was used for the control group. The tumor size and body weight were measured every three days. As shown in Figure 8a, when the mice were treated with normal saline (treated control mice), the tumor volume increased faster than in DOX- and DOX-loaded mPEG-SS-PNLG(90%) micelles-treated mice. At 21 days post-injection, free DOX and the DOX-loaded mPEG-SS-PNLG(90%) micelles formulation reduced

tumor sizes by 71.32% and 39.76%, respectively, compared to the saline-treated mice. The in vivo performance of DOX-loaded mPEG-SS-PNLG(90%) micelles was better than that of free DOX in tumor inhibition. The enhanced tumor inhibition of DOX-loaded mPEG-SS-PNLG (90%) micelles can be attributed to the prolonged circulation, the efficient cell uptake after accumulation at the tumor site via the EPR effect, and the accelerated drug release by the pH- and redox-triggered micelles in the subcellular compartments of the tumor. Nevertheless, free DOX was less effective because of the quick excretion by glomerular filtration.[54] In regards to safety evaluation, as shown in Figure 8b, the treatment with free DOX resulted in the greatest body weight loss (21%) compared with the initial body weight as a result of the severely toxic effects of DOX. In contrast, the treatment with DOX-loaded mPEG-SS-PNLG(90%) micelles appeared to be well-tolerated and did not induce any significant body weight loss. The results indicate that DOX-loaded mPEG-SS-PNLG(90%) micelles exhibited a better antitumor efficacy than free DOX. Importantly, the enhanced survival rate of each formulation was also studied to evaluate the tumor growth inhibition ability of DOX-loaded mPEG-SS-PNLG(90%) micelles **(**Figure 8c**)**. The survival rate of free DOX-treated mice was 75% at 21 days, indicating that treatment with free DOX in tumor-bearing mice resulted in severe toxicity. In contrast, for the mice treated with DOX-loaded mPEG-SS-PNLG (90%) micelles, 87.5% of the animals survived until at least 21 days. It is concluded that the enhanced survival rate of DOX-loaded mPEG-SS-PNLG(90%) micelles-treated mice was likely due to the high therapeutic efficacy and the low toxic effects of polymeric micelles compared to free DOX. After 24 days of treatment with the saline-control, free DOX and DOX-loaded mPEG-SS-PNLG(90%) micelles, the tumor weights were recorded for evaluation of anticancer therapeutic efficacy. Tumor weight was significantly decreased in the mice treated with DOX-loaded mPEG-SS-PNLG(90%) micelles (Figure 8d).

To further evaluate the antitumor efficacy of the DOX-loaded mPEG-SS-PNLG(90%) micelles, histological staining of the excised tumors were performed using H&E and TUNEL assays. For the H&E staining assays **(**Figure 9**)**, fewer tumor cells were observed with DOX-loaded mPEG-SS-PNLG(90%) micelles- treated groups, in comparison to saline-control groups and free DOX- treated groups. Furthermore, the TUNEL assays quantified cell apoptosis in the saline-control, free DOX and DOX-loaded mPEG-SS-PNLG(90%) micelles-treated groups, and the highest level of tumor apoptosis was observed in the group treated with DOX-loaded mPEG-SS-PNLG(90%) micelles. These results clearly confirm that pH and redox dual-responsive DOX-loaded mPEG-SS-PNLG(90%) micelles loaded with DOX provide high antitumor efficacy compared with free DOX.

## 4. Conclusion

We have demonstrated a new type of redox and pH dual-responsive nanosized polymeric micelle with uniform size based on mPEG-SS-PNLG diblock copolymers which are able to efficiently load and deliver DOX into cancer cells, achieving superior anticancer activity. These intelligent biodegradable block copolymers respond to endosomal pH as well as cytoplasmic glutathione for enhanced intracellular anticancer drug release. The empty polymeric micelles are non-toxic to HepG2 cells and the DOX-loaded mPEG-SS-PNLG(90%) micelles possess efficient apoptosis-inducing efficacy against liver cancer cells. Thus, this novel pH and redox dual-responsive mPEG-SS-PNLG diblock copolymer holds great promise for efficient intracellular delivery of potent anticancer drugs, affording enhanced cancer therapeutic efficacy.

## Disclosures

The authors declare no conflict of interest.

**Acknowledgements**

This research was supported by the Basic Science Research Program through a National Research Foundation of Korea grant funded by the Korean Government (MEST) (20100027955) and National Natural Science Foundation of China (NSFC) (No. 51473023).

**References**

1 A. S. Mikhail , C. Allen, *J. Control. Release.,*2009*,* **138**, 214-223.
2 K. Y. Dane, C. Nembrini, A. A. Tomei, J. K. Eby, C. P. O'Neil, D. Velluto, M. A. Swartz, L. Inverardi and J. A. Hubbell, *J. Control. Release.*, 2011, **156**, 154-160.
3 P. Couvreur, *Adv. Drug. Deliv. Rev.*, 2013, **65**, 21-23.
4 A. Eldar-Boock, D. Polyak, A. Scomparin and R. Satchi-Fainaro, *Curr. Opin. Biotech.*, 2013, **24**, 682-689.
5 A. Schroeder, D. A. Heller, M. M. Winslow, J. E. Dahlman, G. W. Pratt, R. Langer, T. Jacks and D. G. Anderson, *Nat. Rev. Cancer.*, 2012, **12**, 39-50.
6 L. Brannon-Peppas and J. O. Blanchette, *Adv. Drug Deliv. Rev.* 2012, **64,** 206-212.
7 F. X. Gu, R. Karnik, A. Z. Wang, F. Alexis, E. Levy-Nissenbaum, S. Hong, R. S. Langer and O. C. Farokhzad, *Nano. Today.*, 2007, **2**, 14-21.
8 K. Greish, *Drug. Discov. Today.*, 2012, **9**, 71-174.
9 J. H. Na, S. Y. Lee, S. Lee, H. Koo, K. H. Min, S. Y. Jeong, S. H. Yuk, K. Kim and I. C. Kwon, *J. Control. Release.*, 2012, **163**, 2-9.
10 X. Duan and Y. Li, *Small*, 2013, **9**, 1521-1532.
11 H. Otsuka, Y. Nagasaki and K. Kataoka, *Adv. Drug. Deliv. Rev.*, 2012, **64**, 246-255.
12 J. M. Harris and R. B. Chess, *Nat. Rev. Drug. Discov.*, 2003, **2**, 214-221.
13 Q. He, Z. Zhang, F. Gao, Y. Li and J. Shi, *Small*, 2011, **7**, 271-280.
14 I. K. Kwon, S. C. Lee, B. Han and K. Park, *J. Control. Release.*, 2012, **164**, 108-114.
15 F. Meng, R. Cheng, C. Deng and Z. Zhong, *Mater. Today*, 2012, **15**, 436-442.
16 V. Torchilin, *Adv. Drug Deliv. Rev.*, 2011, **63**, 131-135.
17 E. Fleige, M. A. Quadir and R. Haag, *Adv. Drug. Deliv. Rev.*, 2012, **64**, 866-884.
18 T. Thambi, V. G. Deepagan, H. Y. Yoon, H. S. Han, S. H. Kim, S. Son, D.G. Jo, C. H. Ahn, Y. D. Suh, K. Kim, I. C. Kwon, D. S. Lee and J. H. Park, *Biomaterials*, 2014, **35**, 1735-1743.
19 Y. Li, G. H. Gao and D. S. Lee, *Adv. Healthc. Mater.*, 2013, **2**, 388-417.
20 H. Y. Yoon, H. Koo, K. Y. Choi, I. C. Kwon, K. Choi, J. H. Park and K. Kim, *Biomaterials*, 2013, **34**, 5273-5280.
21 M. Li, Z. Tang, S. Lv, W. Song, H. Hong, X. Jing, Y. Zhang and X. Chen, *Biomaterials*, 2014, **35**, 3851-3864.

22 C. J. Chen, Q. Jin, G. Y. Liu, D. D. Li, J. L. Wang and J. Ji, *Polymer*, 2012, **53**, 3695-3703.
23 S. de Pedro, V. J. Cadarso, T. N. Ackermann, X. Muñoz-Berbel, J. A. Plaza, J. Brugger, S. Büttgenbach and A. Llobera, *J. Micromech. Microeng.*, 2014, **24**, 125008.
24 Y. J. Pan, Y. Y. Chen, D. R. Wang, C. Wei, J. Guo, D. R. Lu, C. C. Chu and C.C. Wang, *Biomaterials*, 2012, **33**, 6570-6579.
25 W. Chen, P. Zhong, F. Meng, R. Cheng, C. Deng, J. Feijen and Z. Zhong, *J. Control. Release.*, 2013, **169**, 171-179.
26 J. Chen, X. Qiu, J. Ouyang, J. Kong, W. Zhong and M. M. Xing, *Biomacromolecules*, 2011, **12**, 3601-3611.
27 S. Wang, S. Zhang, J. Liu, Z. Liu, L. Su, H. Wang and J. Chang, *Appl. Mater. Inter.*, 2014, **6**, 10706-10713.
28 Z. X. Zhou, Y. Q. Shen, J. B. Tang, M. H. Fan, E. A. Van Kirk, W. J. Murdoch and M. Radosz, *Adv. Funct. Mater.,* 2009, **19**, 3580–3589.
29 M. Q. Li, Z. H. Tang, H. Sun, J. X. Ding and X. S. Chen, *Polym. Chem.,*2013, **4**, 1199-1207.
30 R. Cheng, F. Feng, F. Meng, C. Deng, J. Feijen and Z. Zhong, *J. Control. Release.*, 2011, **152**, 2-12.
31 S. Yu, C. He, J. Ding, Y. Cheng, W. Song, X. Zhuang and X. Chen, *Soft Matter*, 2013, **9**, 2637.
32 L. Wang, W. Cao, Y. Yi and H. Xu, *Langmuir*, 2014, **30**, 5628-5636.
33 W. Chen, P. Zhong, F. H. Meng, R, Cheng, C. Deng and Z. Zhong, *J. Control. Release.*, 2013, **169**, 171-179.
34 Q. N. Bui, Y. Li, M. S. Jang, D. P. Huynh, J. H. Lee and D. S. Lee, *Macromolecules*, 2015, **48**, 4046-4054.
35 J. Chen, X. Z. Qiu, J. Yang, J. Kong, W. Zhong and M. M. Q. Xing, *Biomacromolecules*, 2011, **12**, 3601-3611.
36 H. Y. Yang, M. S. Jang, G. H. Gao, J. H. Lee and D. S. Lee, *Nanoscale,* DOI: 10.1039/C5NR06542A.
37 J. W. Choi, J. Kim, Q. N. Bui, Y. Li, C. O. Yun, D. S. Lee and S. W. Kim, *Bioconjugte Chem*, 2015, **26**, 1818-1829.
38 Y. Li, Y. Shen, S. Wang, D. D. Zhu, B. Du and J. Jiang, *RSC Adv.*, 2015, **5**, 30380-30388.
39 W. Huang, W. Wang, P. Wang, Q. Tian, C. N. Zhang and H. Tang, *Acta Biomaterialia*, 2010, **6**, 3927–3935.
40 C. He, X. Zhuang, Z. Tang, H. Tian and X. *Adv. Health. Mater.*, 2012, **1**, 48-78.
41 L. Zhao, N. Li, K. Wang, C. Shi, L. Zhang and Y. Luan, *Biomaterials*, 2014, **35**, 1284-1301.
42 C. Deng, J. Wu, R. Cheng, F. Meng, H. A. Klok and Z. Zhong, *Prog. Polym. Sci.*, 2014, **39**, 330-364.
43 Y. Li, G. H. Gao, D. S. Lee, *J. Polym. Sci. Pol. Chem.*, 2013, **51**, 4175-4182.
44 J. C. Zhang, L. L. Wu, F. H. Meng, C. Deng and Z.Y. Zhong, *Langmuir*, 2012, **28**, 2056-2065.
45 J. S. Kim, Y. Li, S. W. Kim and D. S. Lee, *Biomaterials*, 2013, **34**, 4622-4631.
46 D. Li, Y. Z. Bu, L. N. Zhang, X. Wang, Y. Yang, H. Shen and D. C. Wu, *Biomacromolecules*, DOI: 10.1021/acs.biomac.5b01394.

47 J. Chen, X. Z. Qiu, J. O. Yang, J. M. Kong, W. Zhong and M. M. Q. Xing, *Biomacromolecules*, 2011, **12**, 3601-3611.
48 T. Thambi and J. H. Park, *J. Biomed. Nanotechnol.*, 2014, **10**, 1841-1862.
49 Y. G. Wang, T. Y. Yang, X. Wang, W. B. Dai, X. Zhang and Q. Zhang, *J. Control. Release.*, 2011, **149**, 299-306.
50 Y. Pan, Y. Chen, D. Wang, and C. Wang, *Biomaterials*, 2012, **33**, 6570-6579.
51 Y. E. Kurtoglu, R. S. Wang, S. Kannan, R, Romero and R. M. Kannan, *Biomaterials*, 2009, **30**, 2112-2121.
52 L. L. Wu, Y. Zou, C. Deng, R. Cheng, F. H. Meng and Z. Y. Zhong, *Biomaterials*, 2013, **34**, 5262-5272.
53 T. Thambi, V. G. Deepagan, H. Ko, Y. D. Suh, G. R. Yi, J. Y. Lee, D. S. Lee and J. H. Park, *Polym. Chem.*, 2014, **5**, 4627-4634.
54 S. J. Yu, J. X. Ding, C. L. He, W. G. Xu and X. S. Chen, *Adv. Health. Mater.*, 2014, **3**, 752-760.

**Table 1. Feed ratios and characteristics of intermediated copolymers mPEG-SS-PBLG**

| Polymer | Reaction time | Molar ratio of initiator/monomer | Degree of polymerization | Mn[a] | Mw[b] | PDI[b] |
|---|---|---|---|---|---|---|
| mPEG-SS-PBLG$_{31}$ | 72h | 1/30 | 31 | 12011 | 11900 | 1.03 |
| mPEG-SS-PBLG$_{41}$ | 72h | 1/40 | 41 | 14201 | 13800 | 1.06 |
| mPEG-SS-PBLG$_{53}$ | 72h | 1/50 | 53 | 16829 | 16600 | 1.08 |

[a] Calculated from $^{1}$H NMR

[b] measured by GPC

**Table 2a. Characteristics and properties of mPEG-SS-PNLG copolymers and micelles (Conversion of benzyl groups in mPEG-SS-PBLG$_{41}$ versus reaction time)**

| Polymer (mPEG-SS-PBLG$_{41}$) | Reaction time | Conversion (%) | Solubility | CMC (mg/mL) | Size[b] (nm) | pKa | Mn[a] | Mw[c] | PDI[c] |
|---|---|---|---|---|---|---|---|---|---|
| mPEG-SS-PNLG(39%) | 12 | 39 | Insoluble | -- | -- | -- | 15225 | 13200 | 1.12 |
| mPEG-SS-PNLG(69%) | 24 | 69 | Not fully soluble | -- | -- | -- | 15993 | 13900 | 1.18 |
| mPEG-SS-PNLG(75%) | 36 | 75 | pH-dependent | 0.026 | 71 | 6.27 | 16121 | 14100 | 1.07 |
| mPEG-SS-PNLG(82%) | 48 | 82 | pH-dependent | 0.024 | 65 | 6.41 | 16313 | 14500 | 1.18 |
| mPEG-SS-PNLG(90%) | 60 | 90 | pH-dependent | 0.023 | 62 | 6.83 | 16505 | 14600 | 1.21 |
| mPEG-SS-PNLG(96%) | 72 | 96 | pH-dependent | 0.020 | 58 | 6.89 | 16761 | 14700 | 1.23 |

**Table 2b. Characteristics and properties of mPEG-SS-PNLG copolymers and micelles (Conversion of benzyl groups in mPEG-SS-PBLG$_{41}$ versus feed molar ratio of 2-(dibutylamino)ethylamine to benzyl groups)**

| Polymer (mPEG-SS-PBLG$_{41}$) | Feed molar ratio of 2-(dibutylamino)ethylamine to benzyl group | Conversion (%) | Solubility | CMC (mg/mL) | Size[b] (nm) | pKa | Mn[a] | Mw[c] | PDI[c] |
|---|---|---|---|---|---|---|---|---|---|
| mPEG-SS-PNLG(12%) | 1:1 | 12 | Insoluble | -- | -- | -- | 14521 | 12300 | 1.29 |
| mPEG-SS-PNLG(39%) | 5:1 | 39 | Insoluble | -- | -- | -- | 15225 | 12900 | 1.18 |
| mPEG-SS-PNLG(70%) | 10:1 | 70 | Not fully soluble | -- | -- | -- | 15993 | 13100 | 1.23 |
| mPEG-SS-PNLG(96%) | 20:1 | 96 | pH-dependent | 0.020 | 58 | 6.89 | 16761 | 14600 | 1.13 |

[a] Calculated from $^1$H NMR

[b] measured by DLS

[c] measured by GPC

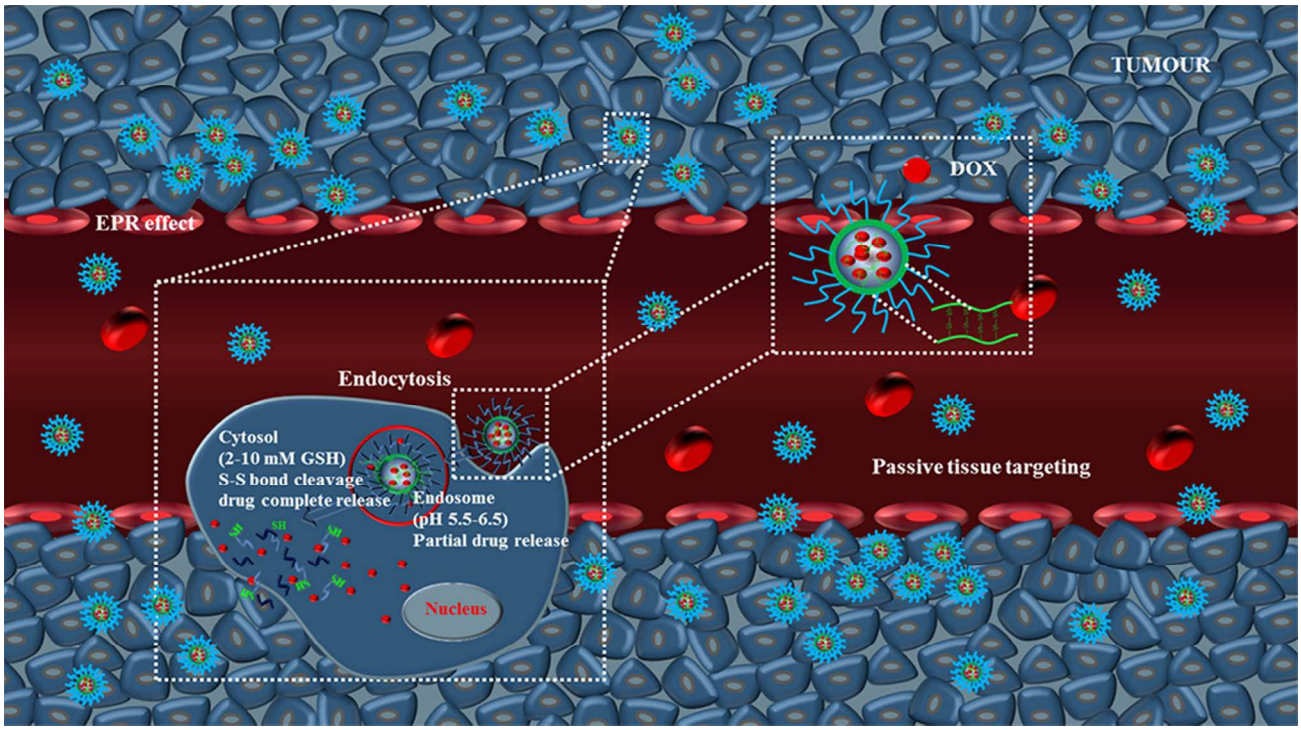


**Scheme 1. Schematic of the complete process of DOX-loaded mPEG-SS-PNLG micelles uptake into tumor cells and intracellular release of DOX.**

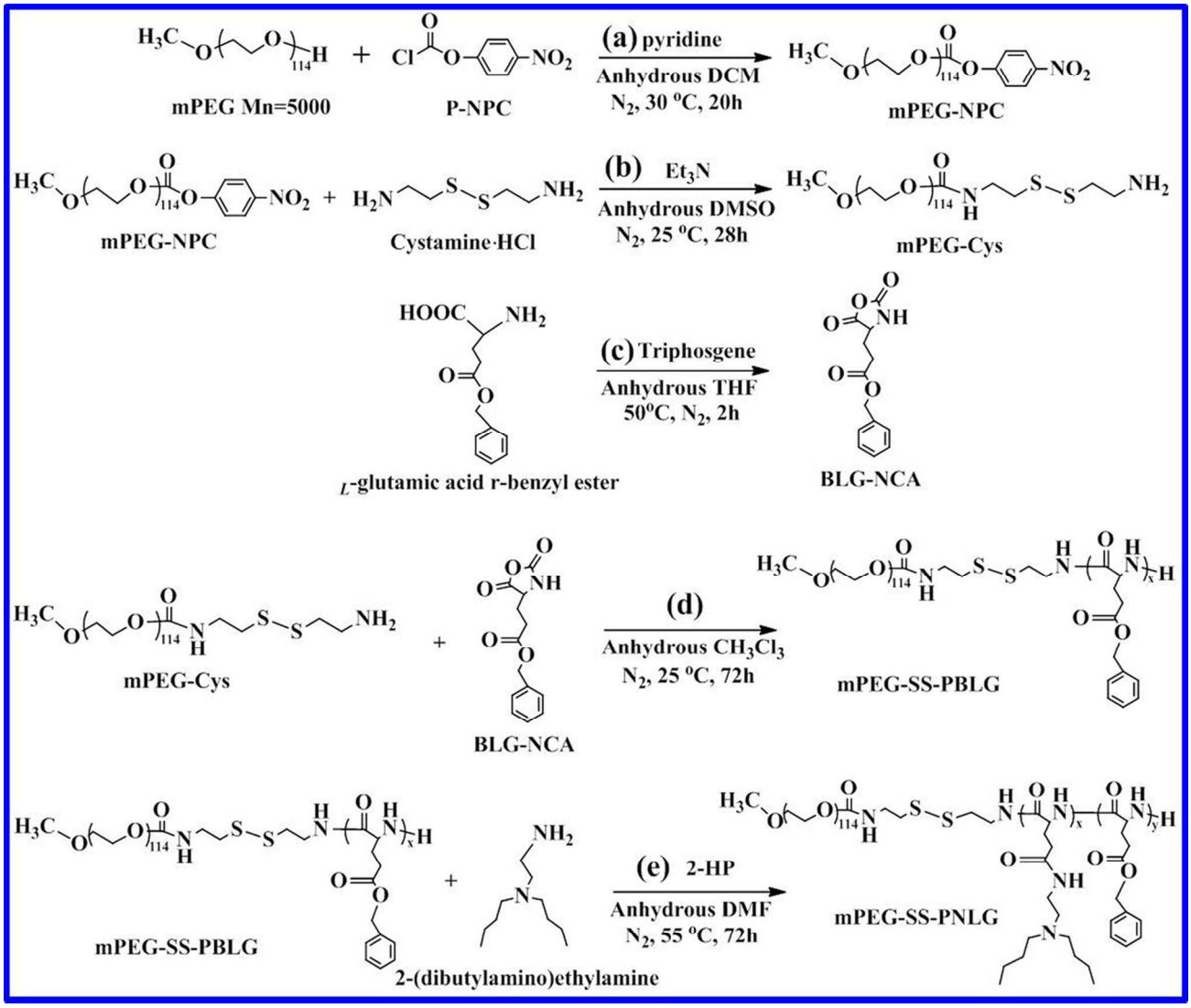


**Scheme 2. Synthesis route of mPEG-NPC (a); mPEG-Cys (b) ; BLG-NCA (c) ; mPEG-SS-PBLG (d) and mPEG-SS-PNLG (e)**

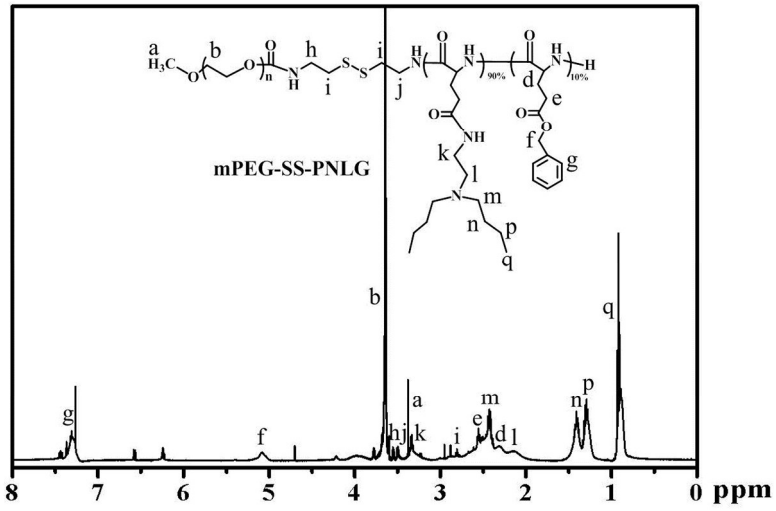


**Fig 1. $^{1}$H NMR spectra of mPEG-SS-PNLG (500MHz, $CDCl_3$)**

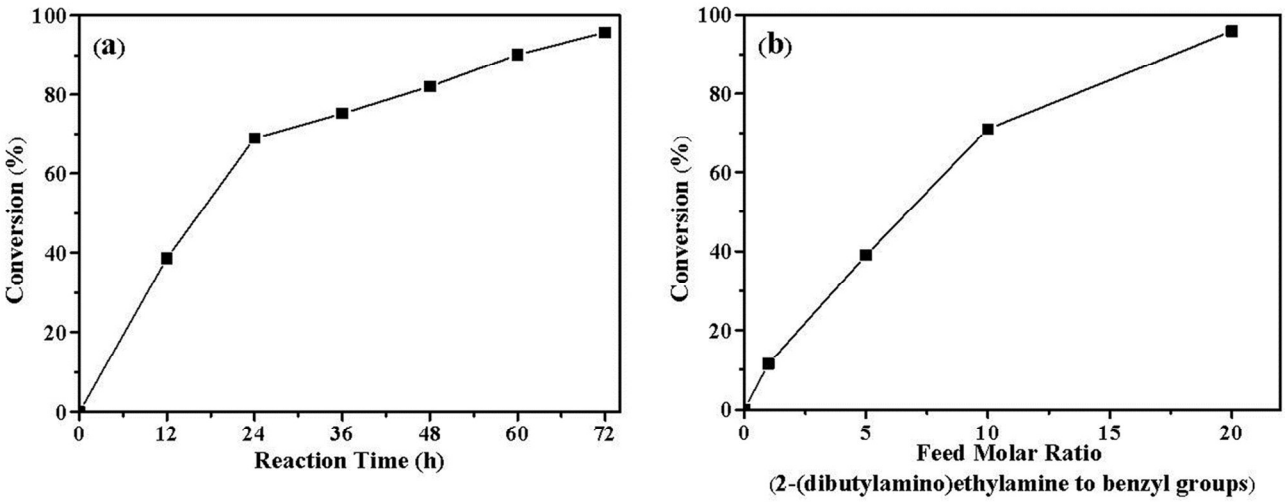


**Fig 2. Conversion of benzyl groups in mPEG-SS-PBLG$_{41}$ versus reaction time (the feed molar ratio of 2-(dibutylamino)ethylamine to benzyl groups is 10:1) (a); versus feed molar ratio of 2 (dibutylamino)ethylamine to benzyl groups (the reaction time for 24 h) (b).**

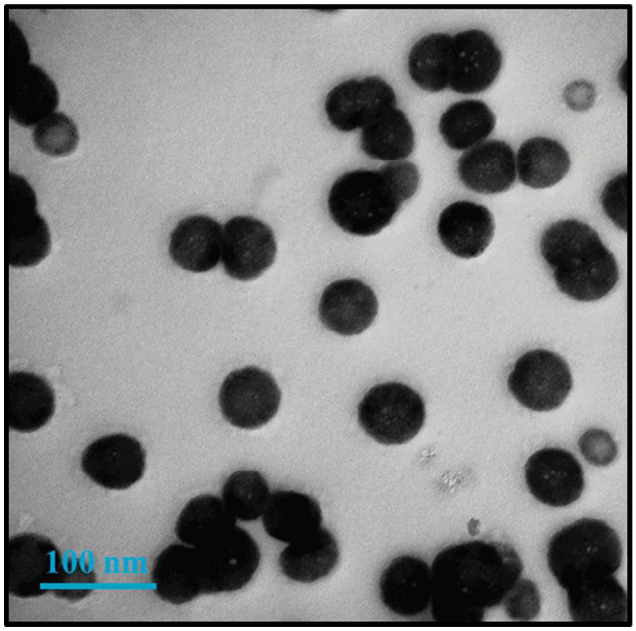


**Fig 3. Size distribution of mPEG-SS-PNLG(90%) micelles determined by TEM**

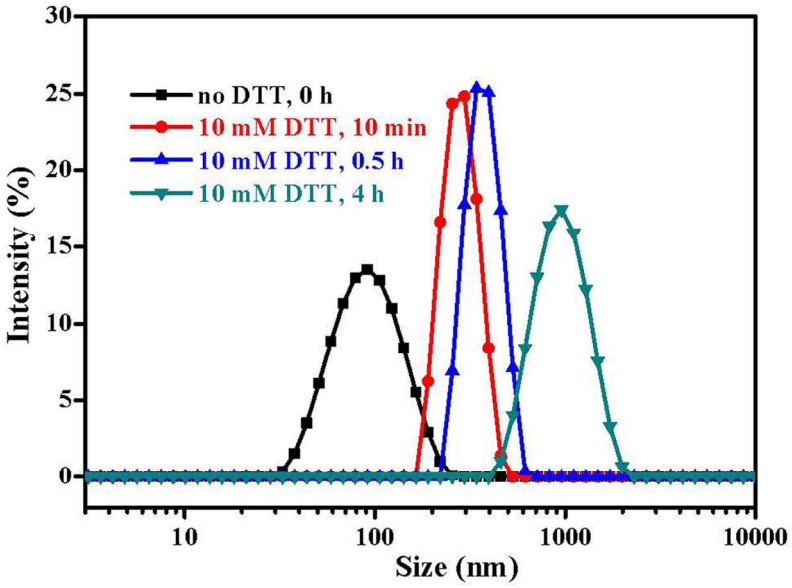


**Fig 4. Redox-induced size change of mPEG-SS-PNLG(90%) micelles solution (1 mg/mL) in different time followed by DLS.**

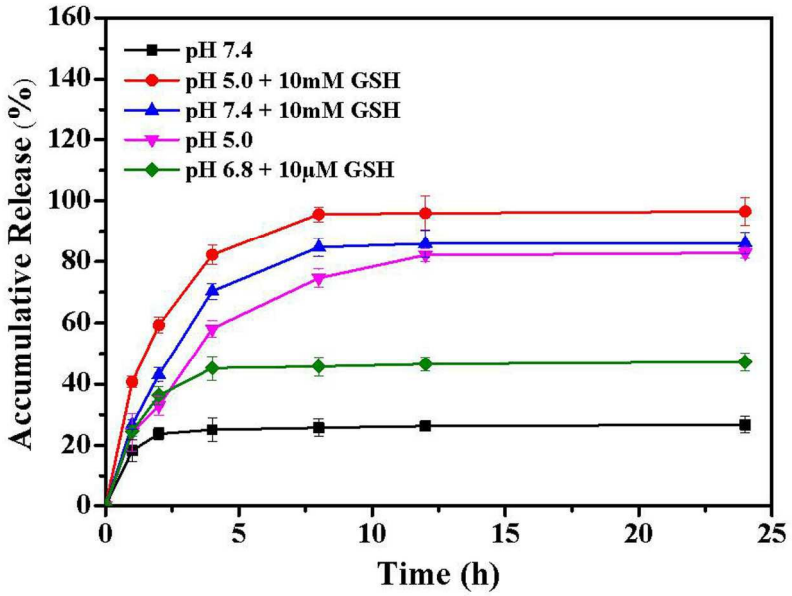


**Fig 5. In vitro drug release profiles of DOX-loaded mPEG-SS-PNLG(90%) micelles in different release media. Data are presented as the mean ± STD (n=3).**

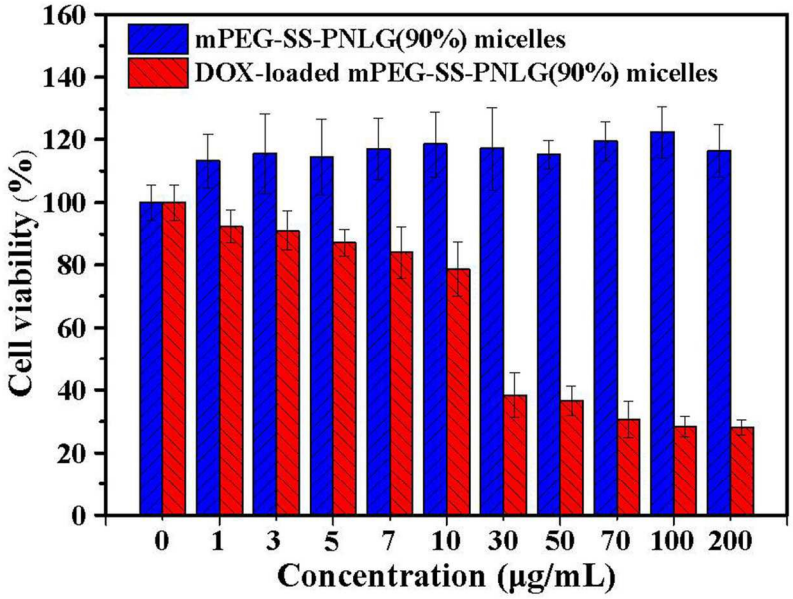


**Fig 6. The in vitro cytotoxicity evaluation of mPEG-SS-PNLG(90%) micelles and DOX-loaded mPEG-SS-PNLG(90%) micelles by an MTT assay.**

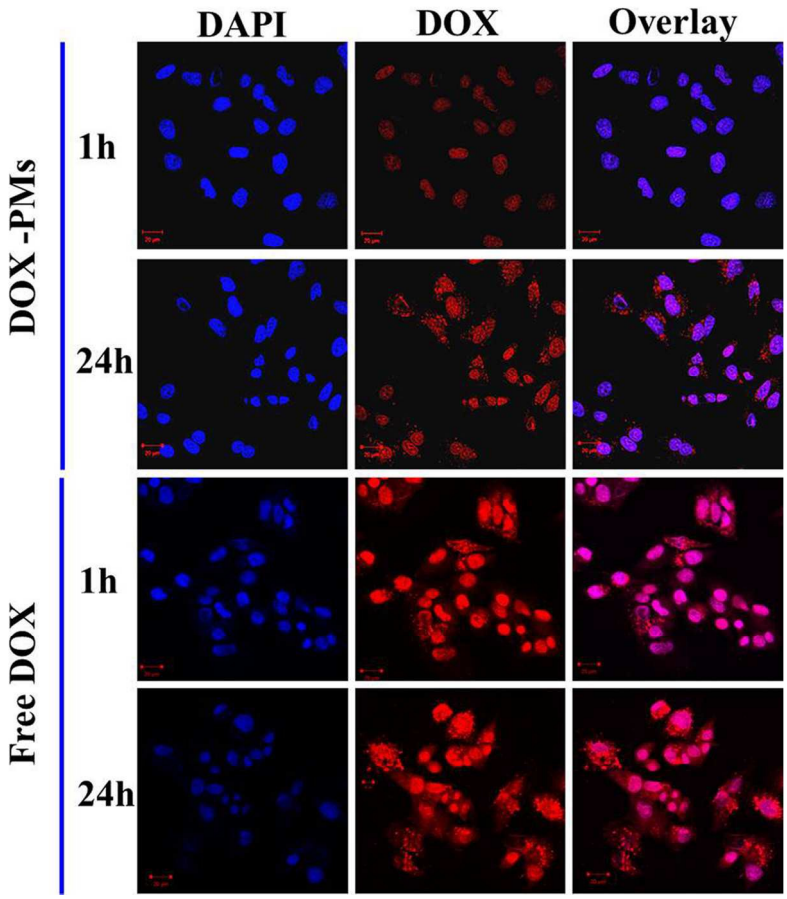


**Fig 7. CLSM images of HepG2 cells following 1 and 24 h incubation with DOX-loaded mPEG-SS-PNLG(90%) micelles (DOX-PMs) and free DOX; The scale bars correspond to 20 μm in all the images.**

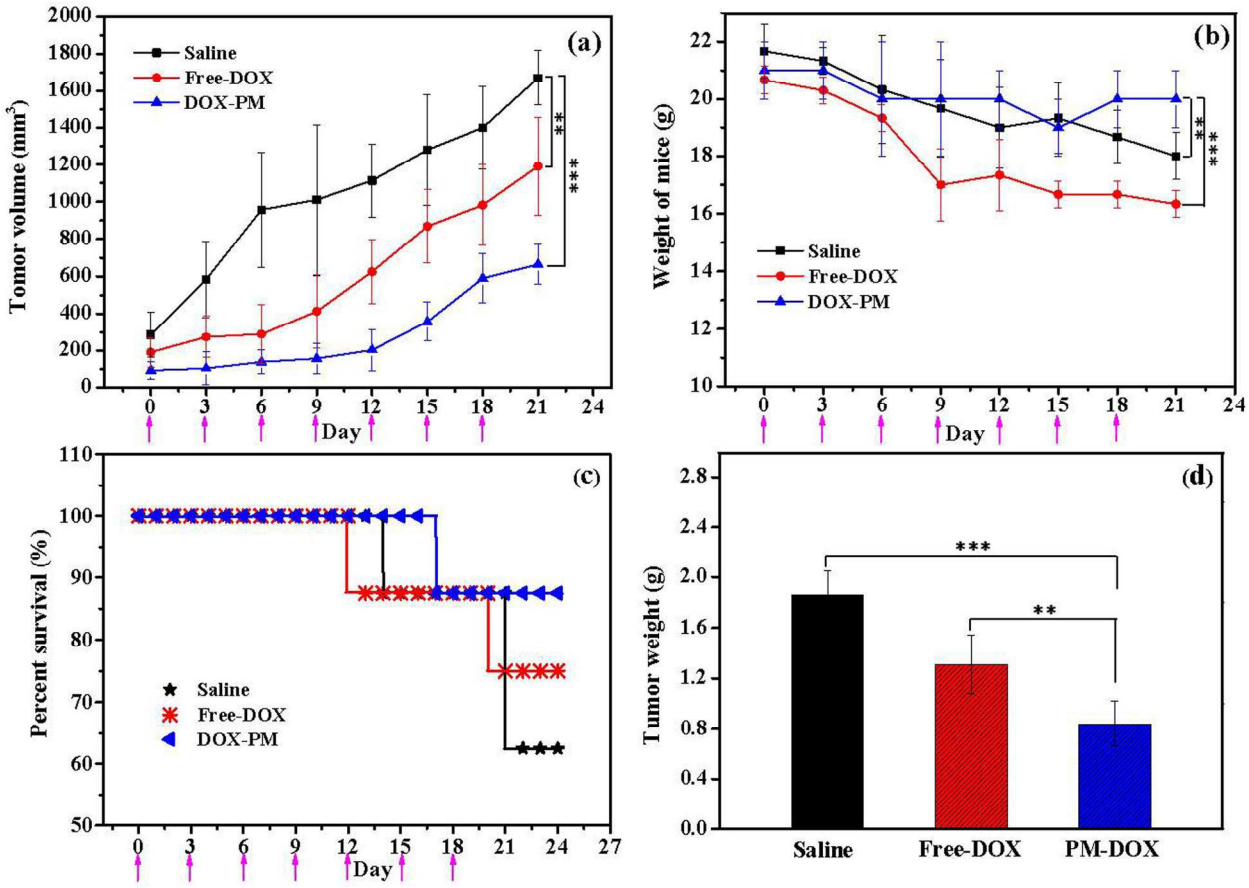


**Fig 8. In vivo antitumor efficacy of Saline (control group), free DOX and DOX-loaded mPEG-SS-PNLG (90%) micelles in the HepG2 liver tumor-bearing mice: (a) Tumor volume of the mice as a function of time; (B) body weight change with the time of tumor bearing mice; (c) survival rate change with the time of tumor bearing mice; (d) tumor weight of mice after treatment. The pink arrow is injection time. The data are shown as mean ± STD (n=8), $^{**}P < 0.01$, $^{***}P < 0.001$.**

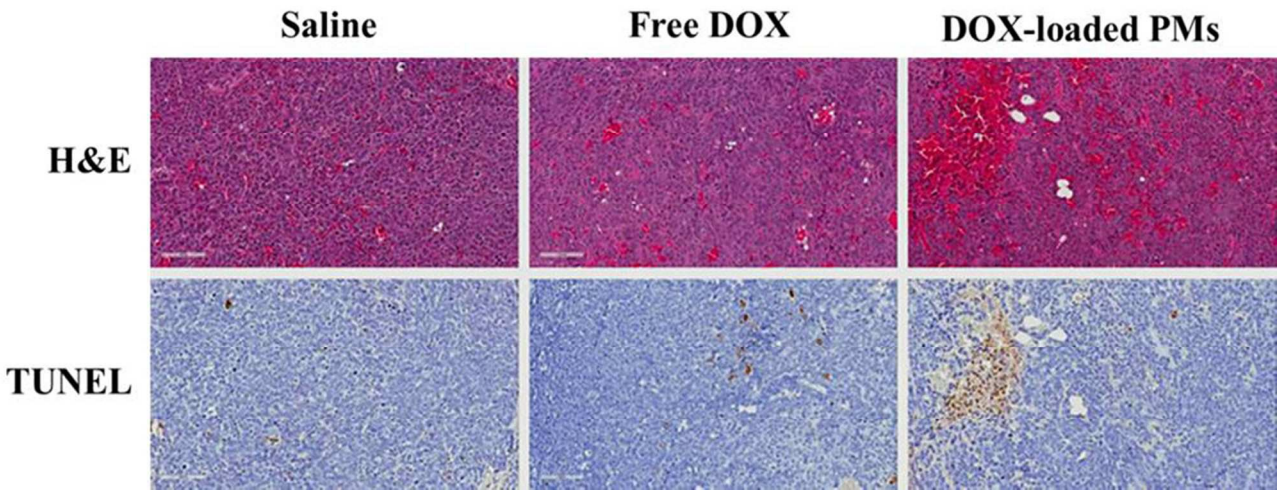


**Fig 9. H&E staining and TUNEL assay of isolated tumor section in HepG2 hepatocellular carcinoma xenograft-bearing nude mice: Saline, Free DOX and DOX-loaded mPEG-SS-PNLG(90%) micelles, respectively.**

**A table of contents entry**

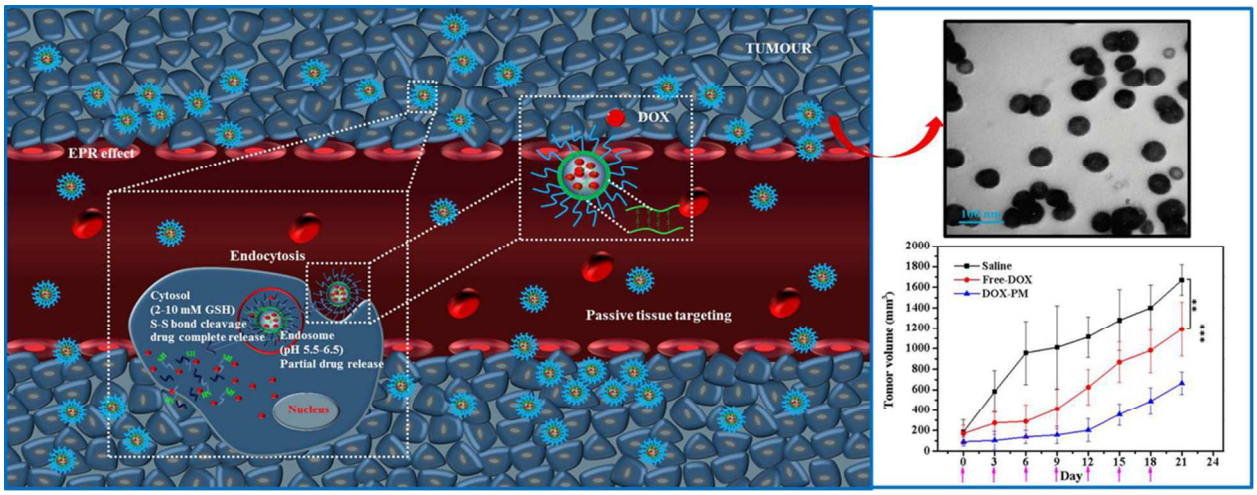


Schematic of the complete process of DOX-loaded mPEG-SS-PNLG micelles uptake into tumor cells and intracellular release of DOX; Size distribution of mPEG-SS-PNLG(90%) micelles and in vivo antitumor efficacy.